

Exploring reaction mechanisms and their competition in $^{58}\text{Ni} + ^{48}\text{Ca}$ collisions at $E = 25 \text{ AMeV}$

L. Francalanza^{1,2}, U. Abbondanno⁴, F. Amorini^{1,2}, S. Barlini⁵, M. Bini⁵, R. Bougault⁶, M. Bruno⁷, G. Cardella³, G. Casini⁸, M. Colonna¹, M. D'Agostino⁷, E. De Filippo³, J. De Sanctis⁷, E. Geraci^{2,3}, A. Giussani⁹, F. Gramegna¹⁰, B. Guiot⁷, V. Kravchuk¹⁰, E. La Guidara¹¹, G. Lanzalone^{12,1}, N. Le Neindre⁶, C. Maiolino¹, P. Marini⁷, L. Morelli⁷, A. Olmi⁸, A. Pagano³, M. Papa³, S. Piantelli⁸, S. Pirrone³, G. Politi^{2,3}, G. Poggi⁵, F. Porto^{2,1}, P. Russotto^{1,2}, F. Rizzo^{2,1}, G. Vannini⁷, L. Vannucci¹⁰

¹ INFN Laboratori Nazionali del Sud – LNS, Catania, Italy

² Dipartimento di Fisica, Università di Catania, Italy

³ INFN Sezione di Catania, Italy

⁴ INFN Sezione di Trieste, Italy

⁵ Dipartimento di Fisica, Università di Firenze, INFN Sezione di Firenze, Italy

⁶ LPC Caen, IN2P3-CNRS/ENSICAEN and Université, F-14050 Caen cedex, France

⁷ Dipartimento di Fisica, Università di Bologna and INFN Sezione di Bologna, Italy

⁸ INFN, Sezione di Firenze, Italy

⁹ Dipartimento di Fisica, Università di Milano and INFN Sezione di Milano, Italy

¹⁰ INFN Laboratori Nazionali di Legnaro, Italy

¹¹ Centro Siciliano di Fisica Nucleare e Struttura della Materia, Catania, Italy

¹² Università Kore, Enna, Italy

Abstract. Latest results concerning the study of central collisions in $^{58}\text{Ni} + ^{48}\text{Ca}$ reactions at $E_{\text{lab}}(\text{Ni})=25 \text{ AMeV}$ are presented. The experimental data, collected with the CHIMERA 4π device, have been analyzed in order to investigate the competition among different reaction mechanisms for central collisions in the Fermi energy domain. The method adopted to perform the centrality selection refers to the global variable “flow angle”, that is related to the event shape in momentum space, as it is determined by the eigenvectors of the experimental kinetic-energy tensor. The main features of the reaction products were explored by using different constraints on some of the relevant observables, such as mass and velocity distributions and their correlations. Much emphasis was devoted to the competition between fusion-evaporation processes with subsequent identification of a heavy residue and a prompt multifragmentation mechanism. The reaction mechanism was simulated in the framework of transport theories (dynamical stochastic BNV calculations, followed by sequential SIMON code) and further comparison with dynamical calculations from transport model (QMD, CoMD) are in progress. Moreover, an extension of this study taking into account for the light particles has been envisaged.

1 Introduction

In heavy ion collisions at intermediate energy (the Fermi energy regime) we can observe phenomena that are characteristic of a transition regime of the reaction mechanisms.

^a Laura Francalanza: laura.francalanza@ct.infn.it

For central collisions, in particular, the competition between prompt multifragmentation processes and sequential particles evaporation or fission-like splitting, after quasi fusion of projectile and target nuclei, plays a relevant role. Multifragmentation of excited heavy systems was characterized by the production of a large average multiplicity of nuclear fragments, more than the one predicted in the de-excitation of an equilibrated excited nuclear system at normal density produced by evaporation in fusion-like reactions [1].

Different scenarios have been proposed in order to explain this new multifragmentation process, counting models that range from prompt dynamical emissions, simulated in the contest of transport theories, to statistical multifragmentation emissions of a low density composite nuclear system at chemical equilibrium.

The experiment was performed by the collaborations NUCLEX and ISOSPIN at LNS – INFN (Catania). A beam of ^{58}Ni isotope was accelerated at the laboratory kinetic energy of 25 AMeV on a thin target of ^{48}Ca by the LNS Superconducting Cyclotron. The reaction products were collected by the 1192 Si-CsI(Tl) telescopes of CHIMERA 4π multidetector [2].

2 Data Selection

In order to perform a good selection of centrality, excluding the most peripheral events from the present analysis, a method based on imposing several cuts on the global variable “flow angle”, θ_{flow} , was used [3-10].

The kinetic flow tensor, Q_{ij} was built starting from the Cartesian coordinates of the measured linear momenta, in the centre of mass frame, for all the fragments ($Z \geq 3$) detected in each event:

$$Q_{ij} = \sum_{Z \geq 3} p_i p_j / 2m$$

(m is the measured mass of each fragment). The diagonal form of the tensor defines an ellipsoid in momentum space with the three principal axes oriented along the three eigenvectors. The orientation of the main axis of the ellipsoid with respect to the direction of the incident beam defines the flow angle θ_{flow} . For peripheral and semi-peripheral collisions, it is possible to imagine an elliptic event shape highly elongated in the beam direction, so that θ_{flow} assumes small values. Otherwise, with increasing centrality more spherical shape is predicted, therefore θ_{flow} will cover a larger range of values, up to 90 degrees.

In fig.1 the longitudinal component (i.e. along the beam axis) of the velocity, v_{par} , versus the mass number of the fragments, A , is shown for different cuts of the flow angle. With increasing the value of the flow angle, we can notice that the contribution from projectile like fragments (PLF) with velocity values close to projectile's velocity ($v_{\text{proj}} = 6.5 \text{ cm/ns}$) and masses around 40-45 amu, is progressively reduced, until it completely vanishes at large values of θ_{flow} , at 60 degrees and beyond. Similar behavior is observed for the contribution of slow moving fragments corresponding to target's remnants, TLF (target like fragment), that are dominant at small flow angle values (close to zero degrees). Both PLFs and TLFs contributions, strongly indicative for binary peripheral collisions, fade away as the flow angle increases.

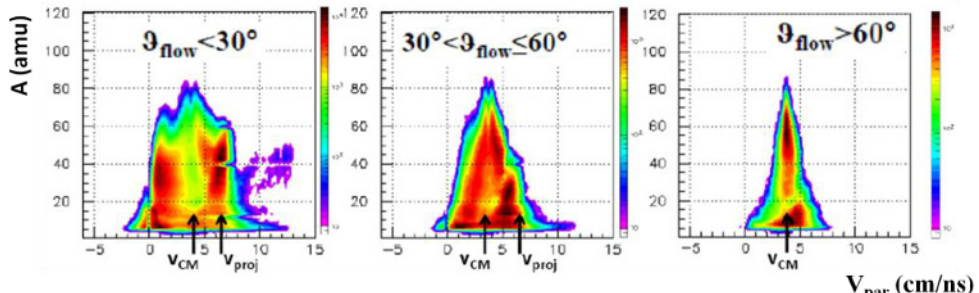


Figure 1. Correlation between parallel velocity component, v_{par} (cm/ns) and mass number A (amu) for all reaction fragments ($Z \geq 3$) in the three regions of flow angle.

In the present work, the data selection results from a cut at θ_{flow} larger than 60° , so focusing the analysis only on those events where peripheral collisions were suppressed. Looking at the results presented in ref.5, we can also notice that an increase in θ_{flow} values results in a selection of more dissipative collisions [11].

3 Qualitative characterization

3.1 Mass – velocity correlation

As we can see by inspecting fig. 1, the region of flow angle larger than 60 degrees shows a longitudinal velocity distribution centered around the centre of mass velocity, v_{CM} , and a relevant emission component due to fragments with mass values greater than those of projectile or target, also exceeding 60 amu. These events, characterized by a low multiplicity of fragments M_{IMF} (IMFs: intermediate mass fragments with $Z \geq 3$), about 1 or 2 per event, represent a strong signature for the formation of a heavy residue coming from fusion-like evaporation processes. Moreover, another kind of emission, with lighter fragments and a larger values of M_{IMF} is present, indicating of the presence of multifragmentation events in the selected data.

3.2 A_{big} analysis

In order to better characterize the selected events with respect to possible competitive mechanisms (fusion-evaporation and multifragmentation) in figure 2 the same velocity – mass correlation plot is reported, only for the heaviest fragment (A_{big}) emitted in each event.

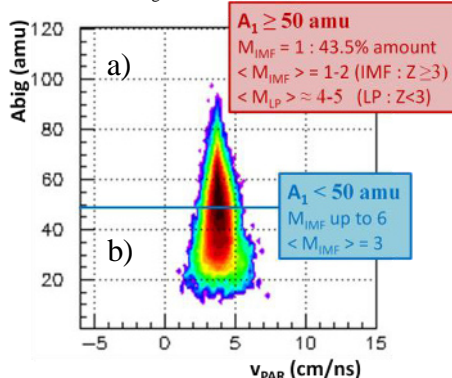


Figure 2. Mass (amu) and longitudinal velocity (cm/ns) for the heaviest fragment for central collisions.

The choice was to analyze two classes of events, imposing preliminarily an arbitrary cut at a value of the mass of the heaviest fragment equal to 50 amu. The heaviest fragment with mass 50 amu or larger is preferentially emitted as a unique heavy fragment (43.5 % of events in figure 2a) in coincidence with 4-5 light charged particles ($Z=1, Z=2$) or, alternatively, together with few light fragments (1-2); in contrast, the fragment multiplicity related to events in figure 2b spans a substantially wider range of values, with a mean of $\langle M_{\text{IMF}} \rangle = 3$, and reaching values as large as $M_{\text{IMF}} = 6$.

Complementary observation of the behavior of the two classes of events come from the analysis of Dalitz plots in figure 3. We briefly remind the reader that each reaction event corresponds to a point in the Dalitz Plot, and that the position of each point (event) inside the triangle gives information about the relative asymmetry in mass of the three heaviest fragments: in the vertices are located events with a heavy residue, the sides are occupied by events characterized by a binary behavior (more or less symmetric splitting) and at the centre of this triangle are located events with a multifragmentation emission of fragments with nearly equal mass. Looking at the left panel of figure 3 (class of events with mass of $A_{\text{big}} \geq 50$ amu) we can observe that most of the events are located on the vertices of the

plot, indicating the dominance of a heavy residue emitted in coincidence with light particles, that displays the characteristic features of typical fusion-evaporation phenomena. Otherwise, events in the right panel (class of events with mass of $A_{\text{big}} < 50$ amu) show the approaching of a more symmetric splitting of the primary source, filling the area inside the triangle and, so, depleting vertices.

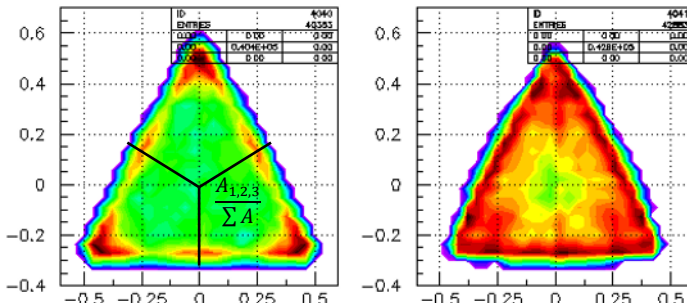


Figure 3. Dalitz Plot for central events.

In ref. 5 preliminary comparisons of the experimental data with the results of a reaction simulations in the frame of stochastic Boltzmann-Nordheim-Vlasov (BNV) model coupled, as second step, with a statistical evaporation model, have shown reasonable qualitative agreement with the assumption of sequential multifragmentation emission [12]. However, to test this preliminary conclusion, further comparisons with dynamical transport models based on different assumptions are needed.

4 Conclusion and perspectives

We have shown experimental information about emission properties of light and heavy fragments produced in central collisions. Much effort was devoted to the characterization of the centrality of the collisions. Multifragmentation of highly excited composite systems appears as a competing mechanism with respect to a sequential emission of fragments produced in fusion-evaporation mechanism. Work is in progress to study fragment-fragment correlation analysis for events with three emitted fragments in the final stage of the reaction. Relative kinetic energy in the centre of mass of the reaction are carefully investigated, taking into account different assumptions of such fragments in the early phase of space-time configuration in order to disentangle between a two step sequential emission from a prompt fragmentation of a unique source (if any). An extension of present analysis to energetic light charged particles is envisaged, in order to investigate relevant characterization of the emitting source.

References

1. W. G. Lynch, Nucl. Phys. A583 (1995) 471-480.
2. A. Pagano," Studies of Nuclear Reactions and Time Scale with the 4π Detector CHIMERA" Nuclear Physics News, 22 25-30 (2012), and references therein.
3. J. Cugnon et al., Nucl. Phys. A 397 519-543 (1983).
4. E. Geraci et al., NPA 732 (2004) 173.
5. L. Francalanza, Il Nuovo Cimento C, 035, 05 (2012).
6. N. Marie et al., Phys. Lett. B391 (1997) 15.
7. M. D'Agostino et al., Phys. Lett B368 (1996) 259.
8. M. Gyulassy et al., Phys. Lett. 110B, 3,4 (1982).
9. Herrman et al., Annu. Rev. Nucl. Part. Sci. 49 581–632 (1999).
10. H. Stocker and W. Greiner, Phys. Rep. 137 277-392 (1986).
11. J. F. Lecolley et al., Phys. Lett B 387 460 (1996).
12. D. Durand, Nucl. Phys. A541, 266 (1992).